Preyssler-Pope-Jeannin Polyanions [NaP5W30O110]14- and [AgP5W30O110]14-: Synthesis, Structural Characterization, Electrochemistry, Antiproliferative and Antibacterial Activity

Haider, A.; Zarschler, K.; Joshi, S. A.; Smith, R.; Lin, Z.; Mougharbel, A.; Herzog, U.; Müller, C. E.; Stephan, H.; Kortz, U.;

Originally published:

August 2018

Zeitschrift für Anorganische und Allgemeine Chemie 644(2018), 752-758

DOI: https://doi.org/10.1002/zaac.201800113

Perma-Link to Publication Repository of HZDR:

https://www.hzdr.de/publications/Publ-27275

Preyssler-Pope-Jeannin Polyanions $[NaP_5W_{30}O_{110}]^{14-}$ and $[AgP_5W_{30}O_{110}]^{14-}$: Microwave-Assisted Synthesis, Structure, and Biological Activity

Ali Haider,[a,d] Kristof Zarschler,[b] Sachin A. Joshi,[a,e] Rachelle M. Smith,[a] Zhengguo Lin,[a,f] Ali S. Mougharbel,[a] Utta Herzog,[b] Christa E. Müller,[c] Holger Stephan,*[b] and Ulrich Kortz*[a]

Dedicated to Professor Peter Comba on the Occasion of his 65th Birthday

Abstract. The Preyssler-Pope-Jeannin polyanion $[NaP_5W_{30}O_{110}]^{14-}$ (**1**) was prepared by microwave-assisted synthesis in only 2 h with a yield comparable to the reported hydrothermal procedure. The purity of **1** was confirmed by FT-IR and multinuclear NMR (^{31}P, ^{183}W) analysis. The silver(I)-containing analogue $[AgP_5W_{30}O_{110}]^{14-}$ (**2**) was also prepared by hydrothermal (6 d) as well as microwave-based (2 h) procedures. Polyanion **2** was characterized in the solid state by FT-IR, single-crystal XRD, TGA, and elemental analysis and in solution by ^{31}P and ^{183}W NMR, and ESI-MS. The antiproliferative activities against human cells as well as the antimicrobial properties towards Gram-positive and Gram-negative bacteria were comparatively evaluated for **1** and **2**.

Introduction

Polyoxometalates (POMs) are discrete anionic metal-oxides of early transition metals in high oxidation states such as V^V, Mo^{VI}, and W^{VI}.[1] POMs have many unique properties that render them of interest for a myriad of applications in diverse areas such as catalysis, magnetism, biomedicine, and materials science.[2] Due to their structural diversity, favorable solubility properties and adjustable stability in biological systems, some POMs have gained interest in medicinal applications, particularly in recent years.[3] Although the molecular mechanism of action is largely unknown, many biological activities of POMs can be attributed to the selective blocking of enzymes at the cell surface.[4] POMs and their inorganic-organic hybrids with antibacterial, antidiabetic, antiproliferative, antiprotozoal, and antiviral activity have been reported.[5] Very recently, the potential of POMs to act as radiosensitizers for treating hypoxic tumors has been recognized.[6]

POMs are usually synthesized via condensation of simple metalate ions in aqueous acidic medium. In such reactions the pH, concentration, temperature, and ionic strength are important parameters.[1] Controlled base hydrolysis can lead to the formation of mono-, di-, tri-, or even hexa-lacunary (defect) precursors which can act as inorganic polydentate ligands for all kinds of metal ions, leading to a large variety of novel POM structures.[1,2] Also, some plenary POMs can act as host templates and encapsulate metal ions, leading to "host-guest" systems. Two common examples of such POM host structures are the cyclic $[P_8W_{48}O_{184}]^{40-}$ ($\{P_8W_{48}\}$) and the donut-shaped $[NaP_5W_{30}O_{110}]^{14-}$ ($\{NaP_5W_{30}\}$).[7] $\{P_8W_{48}\}$ was first reported in 1985 by *Contant* and *Tézé*,[7b] and in 2005 some of us reported the encapsulation of 20 copper(II) ions into the cavity of $\{P_8W_{48}\}$.[8] On the other hand, $\{NaP_5W_{30}\}$ was first reported by *Preyssler* in 1970 and formulated as $(WO_3)_{18}(PO_4)_3H(NH_4)_3$.[7a] In 1985 *Pope* and *Jeannin* reported the actual formula and structure, as based on single crystal XRD.[9] These authors also discovered that the central cavity of $\{NaP_5W_{30}\}$ encapsulates a tightly bound Na^+ ion guest. In 1993, Pope's group demonstrated the exchange of Na^+ by lanthanide ions.[10] This work also inspired others to investigate the host-guest properties of $\{NaP_5W_{30}\}$.[11] More recently, Ca^{2+}, Bi^{3+}, and even two K^+ ions have been encapsulated in this POM host,[12] as well as Ag^+.[13]

$\{NaP_5W_{30}\}$ is not just of interest in terms of exchanging the central Na^+ ion, but it has also been used to form inorganic-

* Dr. H. Stephan
E-Mail: h.stephan@hzdr.de
* Dr. U. Kortz
E-Mail: u.kortz@jacobs-university.de
[a] Department of Life Sciences and Chemistry
Jacobs University
Campus Ring 1
28759 Bremen, Germany
[b] Institute of Radiopharmaceutical Cancer Research
Helmholtz-Zentrum Dresden-Rossendorf
Bautzner Landstraße 400
01328 Dresden, Germany
[c] PharmaCenter Bonn, Pharmaceutical Institute
Pharmaceutical Chemistry I
University of Bonn
An der Immenburg 4
53121 Bonn, Germany
[d] Present address: Department of Chemistry
Quaid-i-Azam University
45320 Islamabad, Pakistan
[e] Present address: Dr. K.C. Patel Research and Development Centre
Charotar University of Science and Technology (CHARUSAT)
Changa Dist., Anand 388421, India
[f] Present address: Key Laboratory of Cluster Science
School of Chemistry and Chemical Engineering
Beijing Institute of Technology
Beijing 100081, P. R. China
Supporting information for this article is available on the WWW under **http://dx.doi.org/10.1002/zaac.201800113** or from the author.

organic hybrids,[14] for catalysis,[4a–4c,15] and for biomedical applications due to its stability at physiological pH.[16] $\{NaP_5W_{30}\}$ is a truly unique and interesting POM, particularly due to its robustness and guest exchange characteristics. However, such reactions in general require high temperatures and long reaction times.[10,12b,17] Some examples of microwave-based synthesis is known in POM chemistry.[18]

Herein we report on a microwave-based procedure for the synthesis of $[NaP_5W_{30}O_{110}]^{14-}$ and the silver(I)-containing derivative $[AgP_5W_{30}O_{110}]^{14-}$, as well as some biomedical studies on both polyanions.

Results and Discussion

Synthesis

Polyanion **1** (Figure 1) was prepared by adding 13.0 mL of 85 % H_3PO_4 dropwise to 15 mL of a 3.34 M Na_2WO_4 solution. The clear solution was stirred under microwave-based conditions (300 W, 1 bar) at 120 °C for 2 h. The resulting solution was cooled to room temperature and 7.5 mL H_2O were added, followed by 5 g KCl in order to precipitate polyanion **1** as a hydrated mixed potassium-sodium salt, $K_{11}Na_3[NaP_5W_{30}O_{110}]\cdot 29H_2O$ (**KNa-1**). For synthetic details see the Experimental Section (vide infra).

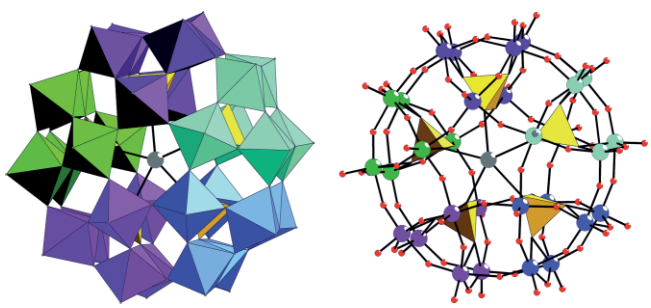

Figure 1. Polyhedral (left) and ball-and-stick (right) representation of the isostructural polyanions **1** and **2**. In **1** the central guest ion (grey ball) is Na^+ and in **2** it is Ag^+. All octahedra (shown in five different colors) represent WO_6 and the PO_4 tetrahedra are shown in yellow. The six WO_6 octahedra of each PW_6 building block are shown in the same color, to highlight the structural nature of the 30-tungsten-5-phosphate shell as a $(PW_6)_5$ pentamer.

Polyanion **2** (Figure 1) was prepared by reaction of $AgNO_3$ solution (3 mL, 0.122 mM) with a solution of **KNa-1** (0.500 g, 0.059 mmol) in 6 mL HNO_3 under hydrothermal heating at 120 °C for 6 d. Addition of KCl (1 g) resulted in the hydrated potassium salt $K_{14}[AgP_5W_{30}O_{110}]\cdot 58H_2O\cdot 2KCl$ (**K-2a**). The detailed chemical composition was confirmed by elemental analysis and TGA (see Experimental Section and Figures S1 and S2 in Supporting Information). The two equivalents of cocrystallized KCl could not be removed by washing steps. We also developed a microwave-based synthetic procedure for the synthesis of **2** (300 W, 1 bar, 120 °C, 2 h stirring). For synthetic details see the Experimental Section (vide infra).

Single crystal XRD analysis revealed that polyanions **1** and **2** are comprised of the well-known donut-shaped 30-tungsto-5-phosphate framework (Preyssler-Pope-Jeannin ion) with either one sodium (**1**) or one silver (**2**) ion located in the central channel (Figure 1). The salt **K-2a** crystallized in the orthorhombic space group *Pnna* (see Table S1 for XRD details, Supporting Information). As expected, the Ag^+ ion in **2** is not located at the exact center of the P_5W_{30} structure, but rather slightly displaced along the fivefold axis. Therefore, the Ag^+ ion guest is crystallographically disordered over two equivalent positions with 50 % occupancies for each, resulting in point group symmetry C_{5v} for **2** (Figure 1). The Ag^+ ion is coordinated to oxygen atoms of the cyclic tungstophosphate host framework with Ag–O bond lengths in the range of 2.560–2.596 Å. The ionic radius of the Ag^+ ion is 1.23 Å (for coordination number 5).[19] The FT-IR spectrum of **2** is rather similar to that of **1**, with some small shifts in the region of 1200–900 cm^{-1}, attributed to the P–O–(Ag) stretching modes.

We have made a large effort trying to optimize the microwave-based reaction conditions for the synthesis of **1** by performing numerous experiments. Finally, the conditions reported herein (120 °C, 2 h) were the best in terms of purity and yield. The same applies for the synthesis of **2** via hydrothermal (120 °C, 6 d) and microwave-based conditions (120 °C, 2 h), respectively. However, for the microwave-based synthesis of **K-2b** a very small **KNa-1** impurity (ca 2–3 %) could not be avoided, as based on ^{31}P NMR (Figure S3, Supporting Information). Attempts to synthesize **2** by direct reaction of WO_4^{2-}, PO_4^{3-}, Ag^+, and K^+ ions remained unsuccessful.

Structural Characterization

In order to efficiently assess the purity of **1** synthesized via microwave-based conditions ^{31}P NMR was used as the key analytical technique (Figure 2).

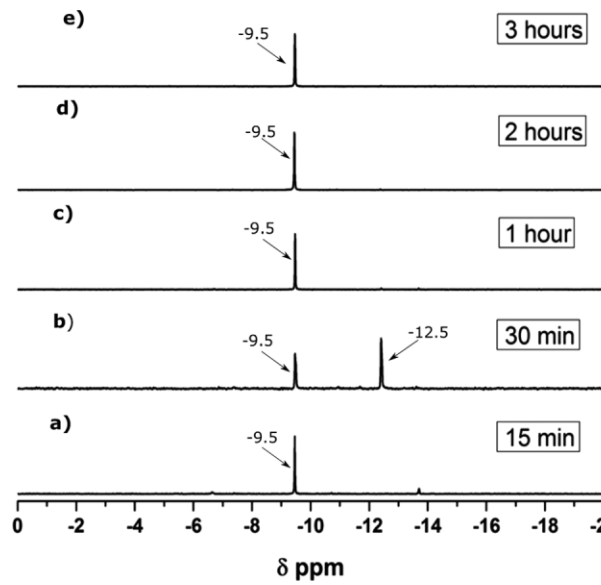

Figure 2. ^{31}P NMR of **KNa-1** prepared via microwave-based synthesis using different reaction times, recrystallized and dissolved in H_2O/D_2O.

All NMR measurements were performed on recrystallized product dissolved in H_2O/D_2O and measured at room tempera-

ture. The full set of results based on time-dependent reactions is summarized in Table S2 (Supporting Information).

It can be seen from the ^{31}P NMR spectra in Figure 2 that polyanion **1** is formed in all reactions, for durations ranging from 15 min to 3 h. Only a singlet at –9.5 ppm is seen, as all phosphorus atoms in **1** are structurally and hence magnetically equivalent.[9,10] The reaction performed for only 15 min (Figure 2a) led to almost pure **1**, but the yield was very low (ca 3 %, see Table S2), suggesting an incomplete reaction. For a reaction time of 30 min a significant impurity signal at –12.5 ppm was observed (Figure 2b), which is assigned to the Wells-Dawson ion $[P_2W_{18}O_{62}]^{6-}$. After 1 h reaction time (Figure 2c) pure **1** was detected, but the yield was only 10 %. After 2 h also pure **1** was obtained with a yield of 20 % (Figure 2d). It should be noted that the reported hydrothermal synthetic procedure of Pope for **1** resulted in 25 % yield in our hands, but after a much longer time (ca 12 h). After 3 h of microwave reaction also pure **1** is formed, but with a decreased yield of 7 % (Figure 2e). Based on these results, a reaction time of 2 h was identified as the best for the microwave-based synthesis of **1**.

In order to further investigate the solution stability and purity of **1**, ^{183}W NMR was performed at 50 °C. The spectrum exhibits the expected four singlets at –201.5, –203.2, –265.1, and –281.3 ppm with relative intensities of 2:2:1:1 (Figure 3). Considering the power of solution ^{31}P NMR, we decided to also monitor the formation of the Ag^+-containing polyanion **2** by this technique. The reactions were performed for different time durations under hydrothermal conditions. When the reaction was performed for 4 d at 120 °C, the desired product **2** was formed (δ = –9.8 ppm), but also some unreacted starting material **1** was present (δ = –9.5 ppm) as well as some unidentified impurity (δ = –8.1 ppm), (Figure 4). Therefore, the reaction was performed for a prolonged time of 6 d. The ^{31}P-NMR of the isolated product showed a clean singlet at –9.8 ppm, corresponding to **2** (as also confirmed by single-crystal XRD). In addition, the hydrolytic stability of **1** and **2** was investigated using absorption spectroscopy. The typical charge-transfer band at about 280 nm (bridging oxygen in W–O–W) remains intact at 25 and 37 °C, indicating the high hydrolytic stability of these polyanions (Figure S4, Supporting Information).

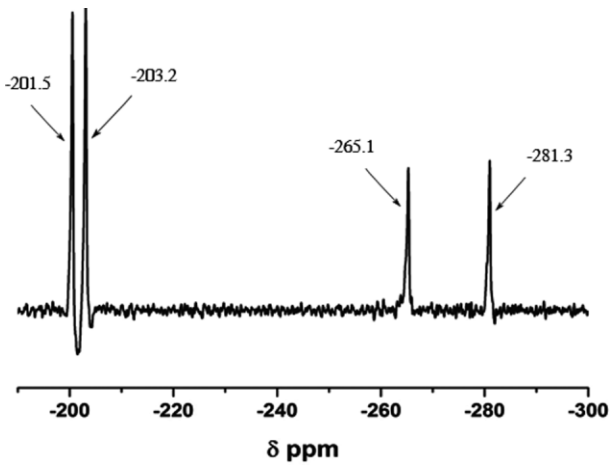

Figure 3. ^{183}W NMR of **KNa-1** dissolved in H_2O/D_2O and measured at 50 °C.

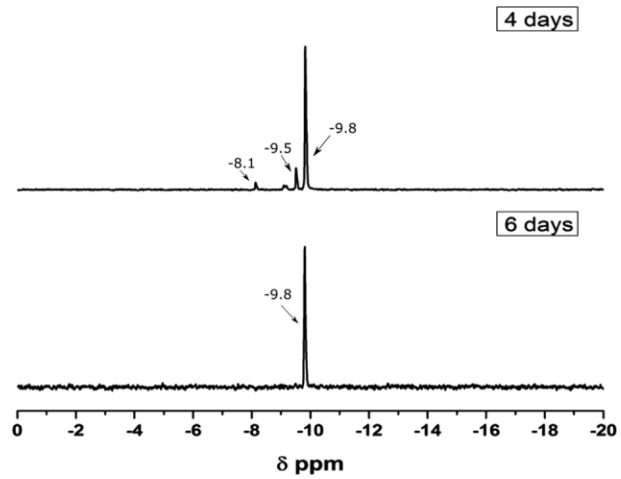

Figure 4. ^{31}P NMR of **K-2a** prepared via hydrothermal synthesis using different reaction times (4 vs. 6 d), recrystallized and dissolved in H_2O/D_2O.

We also performed ^{183}W NMR at 50 °C on **K-2a** dissolved in H_2O/D_2O (Figure 5). The spectrum shows the expected four peaks at –203.4, –205.2, –271.1, and –283.4 ppm with relative intensities of 2:2:1:1, as **2** also has C_{5v} symmetry.

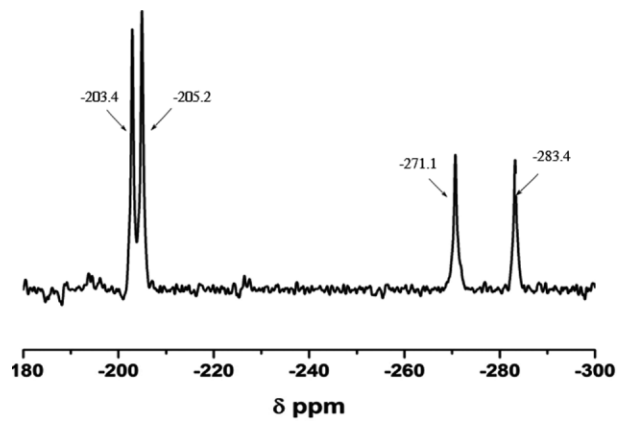

Figure 5. ^{183}W NMR of **K-2a** dissolved in H_2O/D_2O and measured at 50 °C.

Furthermore, we performed ESI-MS studies on **K-2a** in the negative mode and the spectrum is shown in Figure 6. The major peaks are a series of envelopes representing the intact polyanion **2**. The difference in the peaks can be attributed to the water and potassium content of the compound. The smallest peak at m/z = 1078.52 can be assigned to the polyanion assembly $\{H_7[AgP_5W_{30}O_{110}]\}^{7-}$. The largest peak at m/z = 1271.44, 1278.27, 1284.09, and 1209.92 represent the species $\{H_8[AgP_5W_{30}O_{110}(H_2O)_4]\}^{6-}$, $\{KH_7[AgP_5W_{30}O_{110}(H_2O)_4]\}^{6-}$, $\{KH_7[AgP_5W_{30}O_{110}(H_2O)_6]\}^{6-}$, and $\{KH_7[AgP_5W_{30}O_{110}(H_2O)_8]\}^{6-}$, respectively. The remaining peaks at m/z = 1556.89 and 1955.86 represent the assemblies $\{K_2H_7[AgP_5W_{30}O_{110}(H_2O)_8]\}^{5-}$ and $\{K_3H_7[AgP_5W_{30}O_{110}(H_2O)_8]\}^{4-}$, respectively.

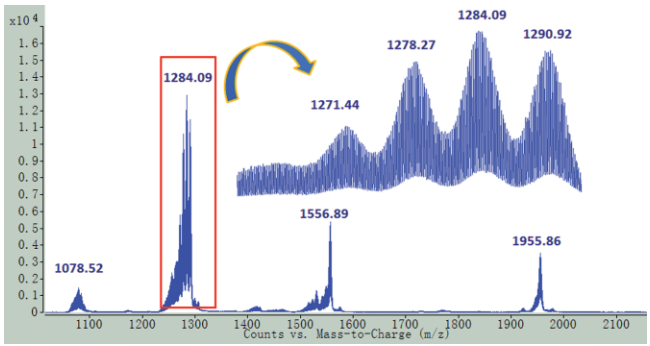

Figure 6. ESI-MS spectrum of **K-2a** in the negative ion mode.

Antiproliferative Studies

The effect of the POM salts **KNa-1** and **K-2a** on the proliferation of the two human cell lines A431 and HEK293 was investigated in a concentration-dependent manner (Figure 7).

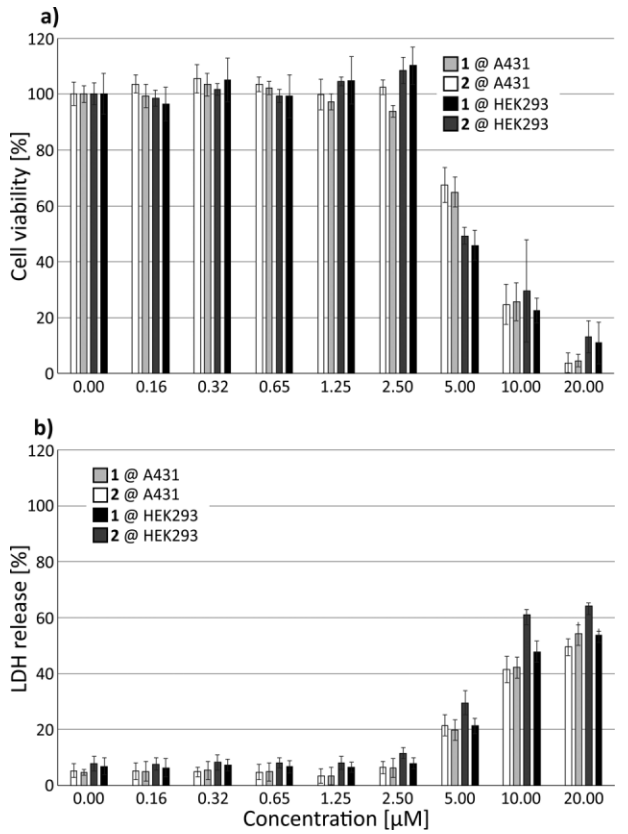

Figure 7. In vitro toxicity evaluation of **1** and **2** after 24 h in A431 and in HEK293 cells. (a) Determination of cellular metabolism as a measure of viability using a MTS assay. The percentage of cell viability is expressed relative to untreated control cells. (b) Determination of membrane integrity by an LDH assay. The percentage of LDH release is expressed relative to LDH release of cells treated with the supplied lysis buffer for maximum LDH release.

Interestingly, these in vitro studies revealed a comparable cytotoxicity of both polyanions after 24 h with IC_{50} values ranging from 7.0 to 7.7 µM, suggesting that the observed cytotoxic effects are independent of the encapsulated guest ion Na^+ vs. Ag^+. *Fu* and co-workers recently reported an IC_{50} value for the human cell line HT29 of 3.6 µM after 36 h of incubation with **1**,[20] which is in agreement with the data obtained herein (Table 1). A reason for these moderate cytotoxic activities could be poor cellular interaction and accumulation of the highly anionic POMs, as their surface charge distribution might prevent sufficient binding to the negatively charged cell membrane.[21] The type of cell death as well as subcellular POM localization and involved target proteins were not further investigated herein, but represent subjects of ongoing research activities. Noteworthy, *Fu* et al. observed a time-dependent increase in the number of apoptotic HT29 cells upon incubation with **1** compared to the untreated control.[20] Most likely, **1** and **2** interact in their intact form with cell membrane constituents such as lipids, receptors or membrane-bound enzymes, thus inhibiting their physiological function and inducing programmed cell death.[4d]

Table 1. IC_{50} values [µM] after 24 h of incubation with **1** and **2**.

	A431	HEK293
1	7.71 ± 1.21	7.69 ± 1.23
2	7.10 ± 0.92	7.05 ± 1.24

Antibacterial Studies

In addition to the cytotoxicity assessment with regard to human cells, the antibacterial activity of the POM salts **KNa-1** and **K-2a** was also evaluated. Gram-negative *E. coli* and Gram-positive *B. subtilis* were chosen as model bacteria for this investigation. The POMs were directly added in a concentration of 1 mg·mL^{-1} to the bacterial media and growth was monitored over time in comparison to bacteria cultivated in the absence of the compounds. As shown in Figure 8, the antimicrobial performance of the Ag-encapsulated POM **2** differs from the bactericidal activity of its Na-containing counterpart **1**. For **2** a general growth inhibitory effect towards both strains

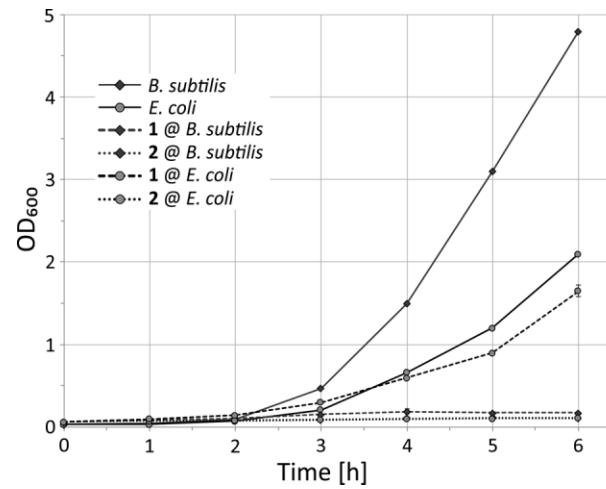

Figure 8. Cell densities measured at a wavelength of 600 nm (OD_{600}) during cultivation of Gram-negative *E. coli* (black) and Gram-positive *B. subtilis* (grey) in the absence (solid lines) and in the presence of 1 mg·mL^{-1} **1** (dashed line) and **2** (dotted line), respectively.

was observed, whereas **1** showed a biocidal effect against Gram-positive *B. subtilis*, but only slightly delayed the growth of Gram-negative *E. coli*. The observed differences in the antibacterial activity of both compounds originate probably from the different cell wall structure between Gram-positive and Gram-negative bacteria as recently described in detail by *Datta* and colleagues.[22] The former prokaryotes possess the very thick peptidoglycan layer, whereas the cell envelope of the latter consists of a thinner peptidoglycan layer in combination with an additional (outer) membrane. As summarized recently by *Rompel* and co-workers, multiple electrostatic interactions between the inorganic POMs and bacterial proteins affecting several biological pathways are mainly responsible for their bactericidal activity.[5f] The underlying antimicrobial mechanism of **1** and **2** as well as investigations on target proteins and processes are part of ongoing studies.

Conclusions

We have successfully synthesized polyanion **1** using a microwave-based procedure in only 2 h, which is much faster than the known hydrothermal procedure (12 h). The purity of **1** was confirmed in the solid state by FT-IR and in solution by ^{31}P and ^{183}W NMR spectroscopy. Furthermore, we have prepared the Ag^+-containing polyanion **2** hydrothermally (as the salt **K-2a**), which was characterized by a multitude of solid- and solution-state analytical techniques. Solution ^{31}P and ^{183}W NMR as well as ESI-mass spectrometry (MS) indicate that **2** is stable. We have also developed a microwave-based procedure allowing synthesizing polyanion **2** (as the salt **K-2b**) in only 2 h.

In vitro studies on **1** and **2** using human cells revealed a dose-dependent inhibition of proliferation and induction of cell death for both polyanions. Interestingly, the Ag^+-containing **2** exhibits an efficient antimicrobial activity against both Gram-positive and Gram-negative bacteria.

Further studies on the incorporation of other guest ions into the Preyssler-Pope-Jeannin polyanion are in progress. With regard to biomedical applications, the preparation of silver-containing POMs allowing for a controlled release of silver ions into the physiological milieu is very attractive.

Experimental Section

Materials and Physical Measurements: All reagents were used as purchased without further purification. All microwave reactions were performed using a CEM Discover XP machine fitted with an IR sensor for temperature control and electromagnetic stirring. Borosilicate vials with a capacity of 35 mL were used. Infrared spectra were recorded as KBR pellets with a Nicolet Avatar 370 FT-IR spectrophotometer. The following abbreviations were used to assign the peak intensities: w: weak; m: medium; s: strong; vs: very strong; b: broad; sh: shoulder. A single crystal suitable for XRD was mounted on a Hampton cryoloop using light oil for data collection at 173 K. Data collection was performed with a Bruker Kappa X8 APEX CCD single-crystal diffractometer with κ geometry and Mo-K_α radiation (λ = 0.71073 Å). The SAINT software suite was used for data integration and processing.[23] The absorption correction was done with SADABS. SHELXS97 was used to locate the W atoms, and successive Fourier syntheses (SHELXL97/2013) allowed to determine the remaining atoms.[24] Thermogravimetric analysis was performed with a TA Instrument Q600 instrument, with sample weights between 10–30 mg in 100 μL alumina pans, in a 100 mL·min^{-1} flow of nitrogen gas, and a heating rate of 5 K·min^{-1}. All NMR measurements were performed with a 400 MHz JEOL instrument with the POMs dissolved in H_2O/D_2O. The ^{31}P NMR measurements were performed in 5 mm tubes at room temperature, whereas the ^{183}W NMR measurements were performed in 10 mm tubes with heating to achieve higher POM concentrations. The respective resonance frequencies were 161.6 MHz (^{31}P) and 16.69 MHz (^{183}W). The chemical shifts are reported with respect to the references 85 % H_3PO_4 (^{31}P-NMR) and 1 M Na_2WO_4 (^{183}W-NMR). Elemental analysis for **K-2a** was performed by Service Central d'Analyse, Solaize, France, and for **KNa-1** and **K-2b** in house by atomic absorption. ESI-MS measurements were performed at the Key Laboratory of Cluster Science in Beijing, China. ESI-mass spectra were obtained in the negative ion mode by using an Agilent 6520 Q-TOF LC/MS mass spectrometer, and the sample solutions were prepared to approximately 10^{-4} M in water and analyzed by direct injection using an automatic sampler with a flow rate of 0.2 mL·min^{-1}. The *m*/*z* values refer to the highest peak in the complex isotopic envelope given by the POM clusters. The dual-spray electrospray ionization source condition was as follows: Vcap: 3500 V; skimmer: 65 V; OCT RfV: 750 V; drying and nebulizer gas: N_2; nebulizer: 30 psi; drying gas flow: 9 L·min^{-1}; drying gas temperature: 300 °C; fragmentator: 80 V; scan range 100–3000 *m*/*z*. Data were accumulated for 500 ms per spectrum. UV absorption spectra were acquired using Analytic Jena Specord 50 spectrometer.

Synthesis of $K_{11}Na_3[NaP_5W_{30}O_{110}]\cdot 29H_2O$ (KNa-1): $Na_2WO_4\cdot 2H_2O$ (16.5 g, 0.05 mol) was dissolved in 15 mL of H_2O under constant stirring and H_3PO_4 (13.0 mL, 85 %) was added dropwise. The clear, colorless solution was placed in a microwave vial fitted with a stir bar and cap, and heated in the microwave for 2 h at 120 °C. The resulting yellow solution was cooled to room temperature. Afterwards 7.5 mL H_2O were added, followed by KCl (5 g) upon stirring. The resulting precipitate was filtered off and washed with 2 M potassium acetate solution and methanol. The dry solid was recrystallized from 15 mL hot water, resulting in a white crystalline product. Yield 2.4 g (17 % based on sodium tungstate). Elemental analysis: calcd. (found): K 5.06 (5.14), Na 1.08 (1.24) %.

Synthesis of $[AgP_5W_{30}O_{110}]^{14-}$ (2):

Procedure 1 (Hydrothermal), $K_{14}[AgP_5W_{30}O_{110}]\cdot 58H_2O\cdot 2KCl$ (K-2a): KNa-1 (0.500 g, 0.059 mmol) was dissolved in 6 mL HNO_3 and heated to approximately 60 °C. Afterwards a solution of $AgNO_3$ (20.7 mg, 0.121 mmol) dissolved in 3 mL H_2O was added dropwise. The cloudy solution was left whilst stirring and heating for 5 min. The mixture was transferred to a 25 mL Teflon liner of a Parr hydrothermal steel reactor and left for 6 d in the oven at 120 °C. When the solution had cooled down to room temperature, KCl (1 g) was added, resulting in a white precipitate, which was recrystallized from water. Yield: 0.30 g (55 % based on **KNa-1**). **IR** (2 % KBr pellet): $\tilde{\nu}$ = 1164 (vs), 1078 (s), 1017 (m), 983 (m), 934 (vs), 785 (vs), 573 (w), 541 (w), 473 (w) cm^{-1} (see Figure S5, Supporting Information). Elemental analysis for **KNa-1**: calcd. (found): K 6.74 (6.78), Ag 1.16 (1.17), P 1.67 (1.76), W 59.44 (59.84) %.

Procedure 2 (Microwave), $K_{14}[AgP_5W_{30}O_{110}]\cdot 22H_2O\cdot 6KCl$ (K-2b): The preparation of the reaction solution was identical to procedure 1 above, but microwave-based heating was used instead of the hydrothermal process. The reaction solution was transferred to a 35 mL mi-

crowave glass vial and kept in the CEM microwave machine at 120 °C and 1 bar pressure for 2 h under constant stirring. When the solution had cooled down to room temperature, KCl (1 g) was added, resulting in a white precipitate, which was recrystallized from water. The IR spectrum of this product was identical to the one prepared via the hydrothermal procedure 1. Yield: 0.30 g (60 % based on **KNa-1**). Elemental analysis for **K-2b**: calcd. (found): K 8.73 (8.71) %.

Cell Culture: Cell culture flasks, dishes and plates (CELLSTARS) were supplied by Greiner Bio-One GmbH. The epidermoid human cancer cell line A431 (ATCCS number: CRL-1555) and the human embryonic kidney cell line HEK293 (DMSZ number: ACC 305) were cultured as previously reported.[25] All cell lines were confirmed to be mycoplasma-negative using the Venor®GeM Advance Mycoplasma Detection Kit (Minerva Biolabs) and were tested monthly.

In vitro Cytotoxicity Evaluation: For the cytotoxicity assessment of polyanions **1** and **2**, MTS (CellTiter 96 Aqueous one Solution Cell Proliferation Assay, Promega) and LDH (Cytoscan™LDH Cytotoxicity Assay, G-Biosciences) assays were performed as detailed previously.[25b] Briefly, 1.8×10^4 A431 or HEK293 cells, respectively, per well were seeded in sterile 96-well microtiter plates. After 24 h incubation, increasing concentrations of either **1** or **2** were added to the cells in quintuplicate. After exposure for 24 h, 10 µL of MTS assay solution were added to the wells and incubated for 1 h. Optical densities at 492 nm were measured with a microplate reader (Sunrise, Tecan). The viability of the cells is expressed as a percentage of viable cells grown in the absence of the POMs. IC_{50} values were calculated using GraphPad Prism 7.04 (GraphPad Software). Additionally, to measure the integrity of the cell membrane, an LDH assay was used in the same cell lines. For this, 1.8×10^4 A431 or HEK293 cells, respectively, per well were seeded in a 96-well microtiter plate. After 24 h incubation, increasing concentrations of either **1** or **2** were added to the cells in quintuplicate and incubated for 24 h. LDH assay solution (50 µL) was added to the cells. Optical density was measured at 492 nm. The percentage of LDH release was expressed relative to LDH release of cells treated with the supplied lysis buffer.

Antibacterial Testing: The antibacterial potential of polyanions **1** and **2** against Gram-negative *E. coli* and Gram-positive *B. subtilis* was assessed by monitoring their growth in LB broth over 6 h in the presence of 1 mg·mL^{-1} of both POMs. Briefly, 200 µL of an overnight culture of each strain were used to inoculate 20 mL of LB broth and cultivation was continued at 37 °C in an orbital shaker with 50 mm offset and shaking speed of 200 rpm (Multitron Cell, Infors). Cell growth was monitored repeatedly by measurement of optical density in 1 mL cuvettes at 600 nm using a spectrophotometer (Ultrospec 10, Biochrom Ltd).

Supporting Information (see footnote on the first page of this article): Thermograms, 31P NMR, absorption and IR spectra, crystal data and details of microwave-assisted synthesis are available on the Internet.

Acknowledgements

U.K. thanks the German Science Foundation (DFG, KO-2288/20–1) and Jacobs University for research support. *A.H.* thanks Deutscher Akademischer Austauschdienst (DAAD) for a doctoral fellowship. We thank *Karin Landrock* for excellent technical assistance.

Keywords: Polyoxometalates; Microwave-assisted synthesis; Nuclear magnetic resonance (NMR); Bioactivity

References

[1] a) M. T. Pope, *Heteropoly and Isopoly Oxometalates*, Springer-Verlag, Berlin Heidelberg, **1983**; b) M. T. Pope, A. Müller, *Angew. Chem. Int. Ed. Engl.* **1991**, *30*, 34–48; c) L. Cronin, in *Comprehensive Coordination Chemistry II* (Ed.: T. J. Meyer), Pergamon, Oxford, **2003**, pp. 1–56; d) M. T. Pope, U. Kortz, in *Encyclopedia of Inorganic and Bioinorganic Chemistry*, John Wiley & Sons, Ltd, **2011**.

[2] a) C. L. Hill, C. M. Prosser-McCartha, *Coord. Chem. Rev.* **1995**, *143*, 407–455; b) P. Gouzerh, A. Proust, *Chem. Rev.* **1998**, *98*, 77–112; c) U. Kortz, A. Müller, J. van Slageren, J. Schnack, N. S. Dalal, M. Dressel, *Coord. Chem. Rev.* **2009**, *253*, 2315–2327; d) O. Oms, A. Dolbecq, P. Mialane, *Chem. Soc. Rev.* **2012**, *41*, 7497–7536; e) S. T. Zheng, G. Y. Yang, *Chem. Soc. Rev.* **2012**, *41*, 7623–7646.

[3] a) J. T. Rhule, C. L. Hill, D. A. Judd, R. F. Schinazi, *Chem. Rev.* **1998**, *98*, 327–358; b) M. Barsukova-Stuckart, L. F. Piedra-Garza, B. Gautam, G. Alfaro-Espinoza, N. V. Izarova, A. Banerjee, B. S. Bassil, M. S. Ullrich, H. J. Breunig, C. Silvestru, U. Kortz, *Inorg. Chem.* **2012**, *51*, 12015–12022; c) K. D. Mjos, C. Orvig, *Chem. Rev.* **2014**, *114*, 4540–4563; d) P. Yang, B. S. Bassil, Z. Lin, A. Haider, G. Alfaro-Espinoza, M. S. Ullrich, C. Silvestru, U. Kortz, *Chemistry* **2015**, *21*, 15600–15606; e) P. Yang, Z. Lin, B. S. Bassil, G. Alfaro-Espinoza, M. S. Ullrich, M. X. Li, C. Silvestru, U. Kortz, *Inorg. Chem.* **2016**, *55*, 3718–3720; f) P. Yang, Z. Lin, G. Alfaro-Espinoza, M. S. Ullrich, C. I. Rat, C. Silvestru, U. Kortz, *Inorg. Chem.* **2016**, *55*, 251–258.

[4] a) F. F. Bamoharram, M. M. Heravi, M. Roshani, M. Jahangir, A. Gharib, *Appl. Catal. A* **2006**, *302*, 42–47; b) F. F. Bamoharram, M. Roshani, M. H. Alizadeh, H. Razavi, M. Moghayadi, *J. Braz. Chem. Soc.* **2006**, *17*, 505–509; c) F. F. Bamoharram, M. M. Heravi, J. Ebrahimi, A. Ahmadpour, M. Zebarjad, *Chin. J. Catal.* **2011**, *32*, 782–788; d) H. Stephan, M. Kubeil, F. Emmerling, C. E. Müller, *Eur. J. Inorg. Chem.* **2013**, 1585–1594; e) S. Y. Lee, A. Fiene, W. Li, T. Hanck, K. A. Brylev, V. E. Fedorov, J. Lecka, A. Haider, H. J. Pietzsch, H. Zimmermann, J. Sevigny, U. Kortz, H. Stephan, C. E. Müller, *Biochem. Pharmacol.* **2015**, *93*, 171–181; f) S. Y. Lee, S. Sarkar, S. Bhattarai, V. Namasivayam, S. De Jonghe, H. Stephan, P. Herdewijn, A. El-Tayeb, C. E. Müller, *Front. Pharmacol.* **2017**, *8*, 54.

[5] a) E. De Clercq, *Rev. Med. Virol.* **2000**, *10*, 255–277; b) E. De Clercq, *Med. Res. Rev.* **2002**, *22*, 531–565; c) B. Hasenknopf, *Front. Biosci.* **2005**, *10*, 275–287; d) M. Aureliano, D. C. Crans, *J. Inorg. Biochem.* **2009**, *103*, 536–546; e) T. Yamase, *Prog. Mol. Subcell. Biol.* **2013**, *54*, 65–116; f) A. Bijelic, M. Aureliano, A. Rompel, *Chem. Commun.* **2018**, *54*, 1153–1169.

[6] Y. Yong, C. Zhang, Z. Gu, J. Du, Z. Guo, X. Dong, J. Xie, G. Zhang, X. Liu, Y. Zhao, *ACS Nano* **2017**, *11*, 7164–7176.

[7] a) C. Preyssler, *Bull. Soc. Chim. Fr.* **1970**, 30–36; b) R. Contant, A. Teze, *Inorg. Chem.* **1985**, *24*, 4610–4614.

[8] S. S. Mal, U. Kortz, *Angew. Chem. Int. Ed.* **2005**, *44*, 3777–3780.

[9] M. H. Alizadeh, S. P. Harmalker, Y. Jeannin, J. Martin-Frere, M. T. Pope, *J. Am. Chem. Soc.* **1985**, *107*, 2662–2669.

[10] I. Creaser, M. C. Heckel, R. J. Neitz, M. T. Pope, *Inorg. Chem.* **1993**, *32*, 1573–1578.

[11] a) M. R. Antonio, L. Soderholm, *Inorg. Chem.* **1994**, *33*, 5988–5993; b) M. H. Dickman, G. J. Gama, K.-C. Kim, M. T. Pope, *J. Cluster Sci.* **1996**, *7*, 567–583; c) M. R. Antonio, C. W. Williams, L. Soderholm, *J. Alloys Compd.* **1998**, *271*, 846–849; d) C. W. Williams, M. R. Antonio, L. Soderholm, *J. Alloys Compd.* **2000**, *303–304*, 509–513; e) M. H. Chiang, M. R. Antonio, C. W. Williams, L. Soderholm, *Dalton Trans.* **2004**, 801–806; f) M. R. Antonio, M. H. Chiang, *Inorg. Chem.* **2008**, *47*, 8278–8285.

[12] a) K. Takahashi, T. Sano, M. Sadakane, *Z. Anorg. Allg. Chem.* **2014**, *640*, 1314–1321; b) A. Hayashi, T. Haioka, K. Takahashi, B. S. Bassil, U. Kortz, T. Sano, M. Sadakane, *Z. Anorg. Allg. Chem.* **2015**, *641*, 2670–2676; c) A. Hayashi, H. Ota, X. Lopez, N. Hiyoshi, N. Tsunoji, T. Sano, M. Sadakane, *Inorg. Chem.* **2016**, *55*, 11583–11592; d) A. Hayashi, M. N. K. Wihadi, H. Ota, X.

López, K. Ichihashi, S. Nishihara, K. Inoue, N. Tsunoji, T. Sano, M. Sadakane, *ACS Omega* **2018**, *3*, 2363–2373.
[13] a) M. X. Liang, C. Z. Ruan, D. Sun, X. J. Kong, Y. P. Ren, L. S. Long, R. B. Huang, L. S. Zheng, *Inorg. Chem.* **2014**, *53*, 897–902; b) C. Kato, K. Y. Maryunina, K. Inoue, S. Yamaguchi, H. Miyaoka, A. Hayashi, M. Sadakane, R. Tsunashima, S. Nishihara, *Chem. Lett.* **2017**, *46*, 602–604.
[14] a) Y. Q. Zhao, K. Yu, L. W. Wang, Y. Wang, X. P. Wang, D. Sun, *Inorg. Chem.* **2014**, *53*, 11046–11050; b) T. P. Hu, Y. Q. Zhao, Z. Jaglicic, K. Yu, X. P. Wang, D. Sun, *Inorg. Chem.* **2015**, *54*, 7415–7423.
[15] a) M. Jiang, D. Zhu, J. Cai, H. Zhang, X. Zhao, *J. Phys. Chem. C* **2014**, *118*, 14371–14378; b) D. M. Fernandes, M. P. Araújo, A. Haider, A. S. Mougharbel, A. J. S. Fernandes, U. Kortz, C. Freire, *ChemElectroChem* **2018**, *5*, 273–283.
[16] a) G. Zhang, B. Keita, C. T. Craescu, S. Miron, P. de Oliveira, L. Nadjo, *J. Phys. Chem. B* **2007**, *111*, 11253–11259; b) H. S. Shah, R. Al-Oweini, A. Haider, U. Kortz, J. Iqbal, *Toxicol. Rep.* **2014**, *1*, 341–352.
[17] A. P. Ginsberg (Editor-in-Chief), *Inorganic Syntheses, Vol. 27*, John Wiley & Sons, Inc., **1990**.
[18] a) A. Bagno, M. Bonchio, A. Sartorel, G. Scorrano, *Eur. J. Inorg. Chem.* **2000**, *2000*, 17–20; b) S. Spillane, R. Sharma, A. Zavras, R. Mulder, C. A. Ohlin, L. Goerigk, R. A. J. O'Hair, C. Ritchie, *Angew. Chem. Int. Ed.* **2017**, *56*, 8568–8572; c) H. Karoui, C. Ritchie, *New J. Chem.* **2018**, *42*, 25–28.
[19] R. Shannon, *Acta Crystallogr., Sect. A* **1976**, *32*, 751–767.
[20] L. Fu, H. Gao, M. Yan, S. Li, X. Li, Z. Dai, S. Liu, *Small* **2015**, *11*, 2938–2945.
[21] K. Y. Wang, B. S. Bassil, Z. G. Lin, A. Haider, J. Cao, H. Stephan, K. Viehweger, U. Kortz, *Dalton Trans.* **2014**, *43*, 16143–16146.
[22] L. P. Datta, R. Mukherjee, S. Biswas, T. K. Das, *Langmuir* **2017**, *33*, 14195–14208.
[23] Bruker, Bruker AXS Inc., Madison, Wisconsin, USA. **2007**.
[24] G. M. Sheldrick, *Program for Crystal Structure Refinement*, University of Göttingen, Germany **1997**.
[25] a) K. Pombo-García, S. Weiss, K. Zarschler, C.-S. Ang, R. Hübner, J. Pufe, S. Meister, J. Seidel, J. Pietzsch, L. Spiccia, H. Stephan, B. Graham, *ChemNanoMat* **2016**, *2*, 959–971; b) K. Pant, J. Pufe, K. Zarschler, R. Bergmann, J. Steinbach, S. Reimann, R. Haag, J. Pietzsch, H. Stephan, *Nanoscale* **2017**, *9*, 8723–8739.

Received: March 29, 2018
Published online: ■